JVI Journals.ASM.org

Sequence of Pathogenic Events in Cynomolgus Macaques Infected with Aerosolized Monkeypox Virus

J. A. Tree, G. Hall, G. Pearson, E. Rayner, V. A. Graham, K. Steeds, K. R. Bewley, G. J. Hatch, M. Dennis, I. Taylor, A. D. Roberts, S. G. P. Funnell, J. Vipond

Microbiological Services, Public Health England, Porton Down, Salisbury, Wiltshire, United Kingdom

ABSTRACT

To evaluate new vaccines when human efficacy studies are not possible, the FDA's "Animal Rule" requires well-characterized models of infection. Thus, in the present study, the early pathogenic events of monkeypox infection in nonhuman primates, a surrogate for variola virus infection, were characterized. Cynomolgus macaques were exposed to aerosolized monkeypox virus (10^5 PFU). Clinical observations, viral loads, immune responses, and pathological changes were examined on days 2, 4, 6, 8, 10, and 12 postchallenge. Viral DNA (vDNA) was detected in the lungs on day 2 postchallenge, and viral antigen was detected, by immunostaining, in the epithelium of bronchi, bronchioles, and alveolar walls. Lesions comprised rare foci of dysplastic and sloughed cells in respiratory bronchioles. By day 4, vDNA was detected in the throat, tonsil, and spleen, and monkeypox antigen was detected in the lung, hilar and submandibular lymph nodes, spleen, and colon. Lung lesions comprised focal epithelial necrosis and inflammation. Body temperature peaked on day 6, pox lesions appeared on the skin, and lesions, with positive immunostaining, were present in the lung, tonsil, spleen, lymph nodes, and colon. By day 8, vDNA was present in 9/13 tissues. Blood concentrations of interleukin 1ra (IL-1ra), IL-6, and gamma interferon (IFN-γ) increased markedly. By day 10, circulating IgG antibody concentrations increased, and on day 12, animals showed early signs of recovery. These results define early events occurring in an inhalational macaque monkeypox infection model, supporting its use as a surrogate model for human smallpox.

IMPORTANCE

Bioterrorism poses a major threat to public health, as the deliberate release of infectious agents, such smallpox or a related virus, monkeypox, would have catastrophic consequences. The development and testing of new medical countermeasures, e.g., vaccines, are thus priorities; however, tests for efficacy in humans cannot be performed because it would be unethical and field trials are not feasible. To overcome this, the FDA may grant marketing approval of a new product based upon the "Animal Rule," in which interventions are tested for efficacy in well-characterized animal models. Monkeypox virus infection of nonhuman primates (NHPs) presents a potential surrogate disease model for smallpox. Previously, the later stages of monkeypox infection were defined, but the early course of infection remains unstudied. Here, the early pathogenic events of inhalational monkeypox infection in NHPs were characterized, and the results support the use of this surrogate model for testing human smallpox interventions.

Since smallpox was declared as being eradicated by the World Health Organization in 1980 (1), laboratory investigations of variola virus have been restricted, leaving a significant gap in the understanding of the immune responses and pathogenesis of this infection (2). Recently, the majority of the human population has not been vaccinated; consequently, a proportion of the population lacks protective immunity (3). Concerns over the use of variola virus or monkeypox virus (a closely related orthopoxvirus) as a biological weapon remain high, as a deliberate release would have catastrophic consequences on global health (4).

The efficacy of therapeutics and vaccines against smallpox cannot be tested in phase III clinical trials in humans, as this is neither ethical nor feasible. Therefore, testing new medical countermeasures requires FDA marketing approval according to the "Animal Rule" (5). Monkeypox virus infection of nonhuman primates (NHPs) presents a potential surrogate disease model for testing intervention strategies for smallpox. Monkeypox virus is related to variola virus and causes a lethal systemic infection in primates. It can also infect humans and presents clinical symptoms similar to those of classic smallpox (6, 7).

Several studies have reported the development of an NHP model of monkeypox virus infection. A variety of challenge routes have been used, including intrabronchial (8), intravenous (8–14), intratracheal (15, 16), intratracheal with MicroSprayer (17), and subcutaneous (18, 19). Natural infection of smallpox usually occurs as a result of close contact with an infected person, via the oropharynx or nasopharynx (20). A deliberate release of variola or monkeypox virus, however, would probably be in aerosol form for rapid dispersion over large areas (21). A limited number of studies have used the aerosol route, characterizing the pathogenic events following aerosol monkeypox virus infection (22–24). Zaucha and

Received 15 October 2014 **Accepted** 26 January 2015

Accepted manuscript posted online 4 February 2015

Citation Tree JA, Hall G, Pearson G, Rayner E, Graham VA, Steeds K, Bewley KR, Hatch GJ, Dennis M, Taylor I, Roberts AD, Funnell SGP, Vipond J. 2015. Sequence of pathogenic events in cynomolgus macaques infected with aerosolized monkeypox virus. J Virol 89:4335–4344. doi:10.1128/JVI.03029-14.

Editor: G. McFadden

Address correspondence to J. A. Tree, julia.tree@phe.gov.uk.

doi:10.1128/JVI.03029-14

colleagues described the systemic dissemination of the monkeypox virus in cynomolgus macaques through a monocytic-cell-associated viremia, similar to that of variola in human beings (23). More recently, two studies described the clinical progression of disease in NHPs following exposure to different doses of aerosolized monkeypox virus (22, 24). These three studies described disease progression from 8 to 17 days after exposure. Pathogenic events earlier than 8 days postinfection have not been reported.

The purpose of this study was to gain a better understanding of the early pathogenic events of monkeypox virus infection following aerosol challenge with a target dose of 10^5 PFU. This study also further characterizes the use of this challenge dose, as used previously, for testing smallpox vaccines (25). In this work, clinical signs of disease, immune cell and antibody responses, viral spread through the body, and pathological changes were examined from days 2 to 12 postchallenge.

MATERIALS AND METHODS

Experimental animals. Twenty-one captive-bred, healthy, male cynomolgus macaques (*Macaca fascicularis*) of Mauritian origin were obtained from a United Kingdom breeding colony. They weighed >2.5 kg and were >2 years of age. All animals were negative for neutralizing antibodies to orthopoxvirus prior to the start of the study. The macaques were housed as required by the United Kingdom Home Office *Code of Practice for the Housing and Care of Animals Used in Scientific Procedures* (26) and the National Committee for Refinement, Reduction, and Replacement (NC3Rs) *Guidelines on Primate Accommodation, Care, and Use* (27). When a procedure required the removal of a primate from a cage, it was sedated by intramuscular (i.m.) injection with ketamine hydrochloride (10 mg/kg of body weight) (Ketaset; Fort Dodge Animal Health Ltd., Southampton, United Kingdom). All procedures were conducted under a project license approved by the local Ethical Review Process of Public Health England, Salisbury, United Kingdom, and the United Kingdom Home Office.

Pathogenesis study. The animals were divided into seven groups of 3 animals and were exposed to aerosolized monkeypox virus on one of two separate occasions with a target dose of 1×10^5 PFU. The mean presented dose was 7.3×10^4 PFU. Animals were scheduled to be euthanized on days 2, 4, 6, 8, 10, and 12 postchallenge. Three animals were designated the reserve group and were used to replace animals that met humane endpoints earlier than their planned necropsy, thus ensuring that 3 animals were available for necropsy at each scheduled time point.

On the day of necropsy, animals were sedated and whole blood and throat swabs collected. For the latter, a flocked swab (Copan Diagnostics, California, USA) was gently stroked 6 times across the back of the throat in the tonsillar area. Viral loads were determined in the blood and throat samples by real-time PCR and plaque assay (see below). The concentration of IgG circulating in the blood was determined by enzyme-linked immunosorbent assay (ELISA; see below). The concentrations of cytokines and the phenotypes of cellular immune populations were determined by Luminex and flow cytometry, respectively (see below). At necropsy, tissues were sampled for histological examination and the determination of viral load by real-time PCR (see below).

Monkeypox virus challenge strain. Monkeypox virus, strain Zaire 79, NR-2324, was obtained from the Biodefense and Emerging Infections Research Resources Repository (BEI Resources, Virginia, USA). On the day of challenge, stocks of virus were thawed and diluted appropriately in minimum essential medium (MEM) containing Earl's salts (Sigma, Poole, United Kingdom), 2 mM L-glutamine (Sigma), and 2% (vol/vol) fetal calf serum (FCS) (Sigma).

Aerosol exposure. Animals were challenged with monkeypox virus using the AeroMP-Henderson apparatus, in which the challenge aerosol was generated using a six-jet Collison nebulizer (BGI, Waltham, MA, USA). This apparatus was designed to deliver a particle size with a mass median diameter of 2.5 μm and a geometric standard deviation of approximately 1.8 (28, 29). The aerosol was mixed with conditioned air in the spray tube (30) and delivered to the nose of each animal via a modified veterinary anesthesia mask. Samples of the aerosol were taken using an SKC BioSampler (SKC Ltd., Dorset, United Kingdom) and an aerodynamic particle sizer (TSI Instruments Ltd., Bucks, United Kingdom); these processes were controlled and monitored using the AeroMP management platform (Biaera Technologies LLC, Maryland, USA). To enable delivery of consistent doses to individuals, each animal was sedated and placed in a "head-out" plethysmograph (Buxco, North Carolina, USA). The aerosol was delivered simultaneously with measurement of the respired volume. A back titration of the aerosol samples taken at the time of challenge was performed to calculate the presented/inhaled dose.

ELISA. Samples of blood were collected at time points throughout the study; serum was separated and assayed for IgG antibodies to vaccinia virus using an ELISA. MaxiSorp 96-well plates (Nunc, Roskilde, Denmark) were coated overnight at 4°C with a preparation of commercially prepared psoralen/UV-inactivated, sucrose density gradient-purified vaccinia virus (Lister strain) (Autogen Bioclear United Kingdom Ltd., Wiltshire, United Kingdom) in calcium carbonate buffer at 2.5 μg ml^{-1}. Unbound antigen was removed by washing the plates 3 times. The plates were treated with blocking buffer (phosphate-buffered saline [PBS], 5% milk powder [Sigma], 0.1% Tween 20 [Sigma]) for 1 h at room temperature with shaking. Unbound blocking solution was removed by washing 3 times with Tris-buffered saline (TBS). Fourfold serially diluted serum samples (starting at 1:50) were added to the plate for 2 h at room temperature, with shaking. Unbound antibodies were removed from the plate by washing 3 times with TBS. The plates were incubated for 2 h, with shaking, with horseradish peroxidase-labeled anti-monkey IgG (Kirkegaard and Perry Laboratories, Maryland, USA). Unbound detection antibody was removed by washing 5 times with TBS and developed using the 2,2′-azino-di-[3-ethylbenzthiazoline sulfonate (6)] (ABTS) peroxidase substrate system (Kirkegaard and Perry Laboratories). The development of the ELISA was stopped by using ABTS stop solution (Kirkegaard and Perry Laboratories). ELISA titers were calculated and compared with a vaccinia immune globulin standard (BEI Research Repository Resource, USA), which was used to convert the titer into arbitrary international units (AIU) per milliliter.

Flow cytometry. Whole blood was collected on days 2, 4, 6, 8, 10, and 12 by using heparin as the anticoagulant. Antibodies to CD3e, CD4, CD20, CD16 (BD Biosciences, Oxford, United Kingdom), and CD8a (Invitrogen, United Kingdom) conjugated to R-phycoerythrin (R-PE)-cyanine dye (Cy7), allophycocyanin (APC), PE, fluorescein isothiocyanate (FITC), and PE-Texas red (TR), respectively, were incubated with the blood for 30 min at room temperature. The red blood cells were removed from the whole blood by lysis with Uti-Lyse reagent (Dako, Cambridgeshire, United Kingdom) and decontaminated overnight with a 4% formaldehyde final concentration solution. Flow count beads (Beckman Coulter, High Wycombe, United Kingdom) were added to provide a standard to enable cell counts per microliter of blood, before being acquired on the flow cytometer. Data were collected on an FC500 flow cytometer (Beckman Coulter) and analyzed with CXP Analysis software version 2.1.

Luminex analysis of cytokines. The concentrations of cytokines were determined in serum samples using an NHP 23-plex kit (Merck Millipore, Massachusetts, USA) according to the manufacturer's instructions. Samples were acquired using a Luminex 200 system (Luminex, Austin, TX, USA), and the data were analyzed using the Xponent software, version 3.0. The concentration of each cytokine in the serum was calculated based on a comparison with the corresponding standard curve generated using purified cytokines from the kit.

Monkeypox virus plaque assay. During the course of the study, EDTA-treated blood and throat swabs were collected and frozen at −80°C. At necropsy, tissues were collected and snap-frozen in liquid nitrogen. Before being tested, tissue was thawed and homogenized in PBS with 1.8-mm ceramic beads in a Precellys24 tissue homogenizer (Ber-

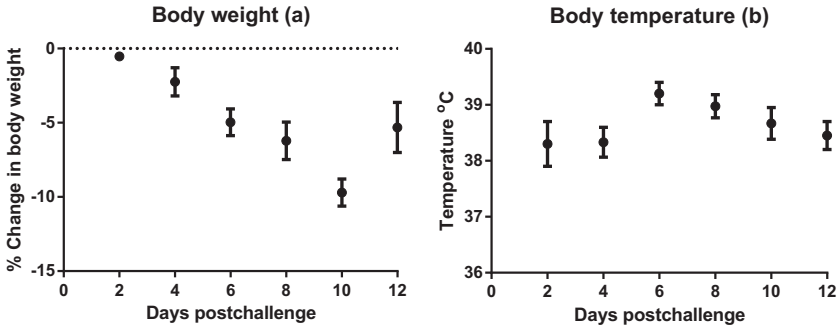

FIG 1 Clinical parameters. (a) Percentage change in body weight; (b) change in body temperature of cynomolgus macaques following aerosol challenge with monkeypox virus (mean ± 1 SE, $n = 3$ to 5 macaques). Body temperature was taken upon euthanasia.

tin Technologies, Villeurbanne, France). The titers of the infectious virus in the tissues, blood, and throat swabs were determined by plaque assay. Samples were incubated in 24-well plates (Nunc; Thermo Fisher Scientific, Loughborough, United Kingdom) with Vero E6 (ATCC CRL-1586; American Type Culture Collection, USA) cell monolayers under MEM (Life Technologies, California, USA) containing 1.5% carboxymethylcellulose (Sigma), 5% (vol/vol) fetal calf serum (Life Technologies), and 25 mM HEPES buffer (Sigma). After incubation at 37°C for 72 h, they were fixed overnight with 20% (wt/vol) formalin-PBS, washed with tap water, and stained with methyl crystal violet solution (0.2% [vol/vol]) (Sigma).

Virus detection by quantitative PCR (qPCR). Tissue samples collected and snap-frozen in liquid nitrogen were defrosted and homogenized in PBS using a Precellys24 tissue homogenizer. Viral DNA was isolated from homogenates using a Qiagen tissue kit (Qiagen, Crawley, West Sussex, United Kingdom) by following the manufacturer's instructions. Blood and throat swabs were processed using a Qiagen blood DNA mini-kit (Qiagen) by following the manufacturer's instructions. Real-time PCR was performed using an Applied Biosystems 7500 Fast instrument (Life Technologies) with an in-house TaqMan assay targeted at the viral hemagglutinin (HA) gene, residues 158734 to 158798, inclusive, in the Z79 genome (GenBank accession no. HQ857562.1, strain V79-I-005).

Clinical and euthanasia observations. Clinical observations were made and scored every 4 to 6 h postchallenge. A scale was used to define disease severity (0 = none, 1 = mild, 2 = substantial, 3 = intense), based on observations that included rectal temperature, body weight, behavioral changes (depression/unresponsiveness/repetitive activity), nasal discharge, cough, dyspnea, and rash/skin swelling. In order to meet the requirement of the project license to limit suffering of animals and identify an endpoint for euthanasia, the clinical well-being of each subject was assessed using a euthanasia scoring scheme which included observations of >20% loss in body weight, convulsions, hemorrhagic rash, and persistent prostration.

Necropsy procedures. Animals were anesthetized with ketamine hydrochloride (20 mg ml^{-1}, i.m.) (Fort Dodge Animal Health Ltd.), and exsanguination was effected via cardiac puncture, followed by injection of an anesthetic overdose (Dolelethal, 140 mg/kg; Vetquinol United Kingdom Ltd.) to ensure euthanasia. A necropsy was performed immediately after confirmation of death.

Pathological studies. At necropsy, abnormalities were recorded and samples were collected from lung lobes, trachea, heart, liver, kidneys, spleen, tongue, tonsil, esophagus, stomach, ileum, descending colon, lymph nodes (tracheobronchial, axillary, mesenteric, mandibular, and inguinal), adrenal gland, ovary or testis, skin (with and without lesion), and brain and placed in 10% neutral buffered formalin. Fixed tissues were processed to paraffin wax, and 5-μm sections were cut and stained with hematoxylin and eosin (H&E). For immunohistochemistry, formalin-fixed, paraffin-embedded tissue sections were mounted on positively charged X-tra adhesive slides (Leica Biosystems, United Kingdom), deparaffinized, and rehydrated. Immunohistochemical staining was achieved using a BOND-MAX immunostainer (Leica Microsystems, United Kingdom) and a Leica Bond Polymer Refine detection kit (Leica Biosystems, United Kingdom). A heat-induced epitope retrieval cycle with buffer ER2 (Leica Biosystems, United Kingdom) was applied for 20 min, followed by a peroxide block for 5 min (Leica Biosystems). Incubation was then performed with a mouse monoclonal antivaccinia antibody (ViroStat, USA) at a dilution of 1:1,800, followed by the post-primary antibody for 8 min (Leica Biosystems). Hematoxylin was used as the counterstain. Positive- and negative-control slides were included. Immunolabeled slides were evaluated using light microscopy.

RESULTS

Clinical signs. Clinical observations from the animals necropsied on days 2 ($n = 3$) and 4 ($n = 3$) scored 0, similar to preexposure levels. Euthanasia scores and body weights (Fig. 1a) remained similar to preexposure levels. On day 4, three animals (from other groups) began to cough. On day 6, signs of acute disease were noted that included increased weight loss, dyspnea, anorexia, and a peak in body temperature (mean, 39.2°C; $n = 3$ animals) (Fig. 1b). On day 8, animals showed signs of severe illness; additionally, two animals from the "reserve group" met the euthanasia criteria on day 8, thus the group size for necropsy on day 8 was $n = 5$ animals. Day 8 was the peak time for clinical signs; coughing was reported for 10 out of 12 animals, and the mean loss in body weight was −9.7% (Fig. 1a). By day 12, surviving animals were showing signs of recovery, with only one animal still coughing. The remaining animal from the "reserve group" was euthanized on day 12; hence, the sample size was $n = 4$ animals.

Enlargement of the lymph nodes (lymphadenopathy) was observed at necropsy in all animals from day 2 onward (see the detailed description in the "Pathology" section below).

The skin of the animals on days 2 and 4 were normal. Pox lesions appeared on day 6 (mean lesion count = 5, range = 0 to 16, $n = 3$ animals). The peak number of lesions occurred on day 8 (mean lesion count = 52, range = 0 to 189, $n = 5$ animals). The mean number of lesions decreased by day 10 (mean lesion count = 45, range = 17 to 70, $n = 3$ animals) and remained similar on day 12 (mean lesion count = 47, range = 4 to 92, $n = 4$ animals).

Immunophenotyping. The changes in absolute counts of different populations of immune cells, in the whole blood, are shown in Table 1. Compared to baseline levels, by day 2 postinfection, there were reductions in lymphocytes ($-2 \times 10^6 ml^{-1}$), $CD4^+$ T cells ($-4 \times 10^5 ml^{-1}$), $CD8^+$ T cells ($-2 \times 10^5 ml^{-1}$), $CD3^+$ T

TABLE 1 Changes in immune populations

Day postchallenge	Cellular population change (cells × 10^3 ml^{-1})[a]													
	Lymphocytes		$CD4^+$ T cells		$CD8^+$ T cells		$CD3^+$ T cells		NK cells		B cells		Monocytes	
	Mean	±1 SE	Mean	±1 SE	Mean	±1 SE	Mean	±1 SE	Mean	±1 SE	Mean	±1 SE	Mean	±1 SE
2	−1,607	606	−398	184	−160	63	−626	267	−132	40	−508	315	−141	7
4	−794	169	−64	75	−60	15	−197	84	−13	17	−278	78	75	83
6	−4,782	3,210	−851	240	−370	156	−1,397	444	−254	121	−625	170	−25	76
8	427	471	−136	142	46	131	−417	279	−60	65	−186	152	262	121
10	2,329	842	186	589	796	181	−77	1348	−66	67	−448	316	556	364
12	1,298	1,225	201	354	645	293	1,636	864	−34	84	−450	293	102	105

[a] Mean absolute cell counts (cells × 10^3 ml^{-1}) in different populations (+ 1 SE; $n = 3$ to 5 macaques) compared to baseline levels (average from two bleeds, taken on different days, prior to challenge) in whole blood, following challenge with aerosolized monkeypox virus.

cells ($-6 \times 10^5 ml^{-1}$), NK cells ($-1 \times 10^5 ml^{-1}$), B cells ($-5 \times 10^5 ml^{-1}$), and monocytes ($-1 \times 10^5 ml^{-1}$). By day 4, cell counts started to rise but remained below baseline levels, except for monocytes, which rose above prechallenge counts ($+7.5 \times 10^4$ ml^{-1}) (Table 1). A second reduction in most immune cells was noted on day 6, followed by a steady rise until day 10 (Table 1). A positive increase was seen in lymphocytes (notably $CD8^+$ T cells) and monocytes on days 8, 10, and 12 ($CD4^+$ T cells rose above baseline from day 10 onward).

Cytokine responses. On day 2, a rise in interleukin 8 (IL-8) (increase of 567 pg ml^{-1}) was seen compared to prechallenge levels, and other biomarkers either decreased (e.g., monocyte chemoattractant protein 1 [MCP-1], IL-12/23, and IL-2) or remained unchanged (Table 2). On day 4, there were increases in the concentrations of gamma interferon (IFN-γ), IL-1ra, IL-6, IL-8, MCP-1, vascular endothelial growth factor (VEGF), IL-18, and IL-2. The concentrations of some cytokines, e.g., IFN-γ (1,322 pg ml^{-1}), IL-1ra (3,335 pg ml^{-1}), IL-6 (570 pg ml^{-1}), IL-8 (2,546 pg ml^{-1}), and MCP-1 (726 pg ml^{-1}), peaked on day 8. Small peaks in the concentrations of other biomarkers, e.g., tumor necrosis factor alpha (TNF-α), IL-1β, macrophage inflammatory protein 1β (MIP-1β), and IL-12/23, occurred on day 10. In contrast, small rises in granulocyte-macrophage colony-stimulating factor (GM-CSF) and IL-10 occurred later, by day 12 (Table 2).

Humoral immune responses. The levels of IgG serum antibodies in the blood to vaccinia virus, determined by ELISA, were increased from day 10 onward (Fig. 2).

Viral load. Viral DNA was first detected in the throat (3.4×10^4 copies ml^{-1}) on day 4. The concentration increased to 9.5×10^5 copies ml^{-1} on day 8 and remained high until the last study day (day 12) (Fig. 3). In contrast, viral DNA (vDNA) was first detected in the blood (8.3×10^3 copies ml^{-1}) on day 8, and its concentration rose to 4.5×10^5 copies ml^{-1} on day 10 and returned to 1.1×10^4 copies ml^{-1} by day 12 (Fig. 3). Viral PFU were detected in throat swabs (above the limit of detection = 25 PFU ml^{-1}) from day 4 to day 12, and a peak in the infectious virus concentration was detected on day 8 (1.4×10^3 PFU ml^{-1}). No

TABLE 2 Serum cytokine profiles of cynomolgus macaques taken during the pathogenesis study

Biomarker	Change in concn of biomarker (pg ml^{-1}) by day postchallenge[a]											
	Day 2		Day 4		Day 6		Day 8		Day 10		Day 12	
	Mean	±1 SE	Mean	±1 SE	Mean	±1 SE	Mean	±1 SE	Mean	±1 SE	Mean	±1 SE
IFN-γ	−2	1	212	55	842	250	1,322	210	380	168	32	13
IL-1ra	−2	4	52	8	313	173	3,335	3,200	18	15	21	7
IL-6	−1	0.3	43	22	213	88	570	339	70	29	17	3
TNF-α	0	0	0	0	2	2	1	1	15	11	1	1
IL-8	567	754	1,186	1,067	193	499	2,546	1,112	1,458	1,511	671	373
IL-1β	0	0	0	0	0	0	1	1	7	6	1	1
MCP-1	−131	64	383	78	651	413	726	93	201	105	132	103
MIP-1α	0	0	0	0	0	0	0	0	1	1	0	0
VEGF	−6	3	6	3	27	11	59	12	20	8	15	9
GM-CSF	0	0	0	0	0	0	1	0.4	1	1	7	7
MIP-1β	−2	1	−1	0	0.3	1	2	1	13	8	3	3
Il-5	−2	1	1	1	−0.3	0.3	1	1	6	3	1	0.5
IL-13	0	0	0	0	0	0	0.2	0.2	2	2	0.3	0.3
IL-10	−1	0	−0.3	0.3	−1	0	0	0.8	3	3	4	4
IL-12/23	−22	11	−5	10	−37	8	−68	13	69	80	46	44
IL-15	−2	1	−1	0.3	3	1	0	1	2	3	−1	1
IL-17	0	0	0	0	0	0	0.2	0.2	0	0	0	0
IL-18	−4	1	4	1	2	3	6	2	3	2	2	0.4
IL-2	−18	2	16	4	17	7	26	5	6	9	9	6

[a] Mean concentration (pg ml^{-1}) (+1 SE; $n = 3$ to 5 macaques) change in cytokine levels compared to baseline levels (average from two bleeds, taken on different days, prior to challenge) on various days following challenge with aerosolized monkeypox virus.

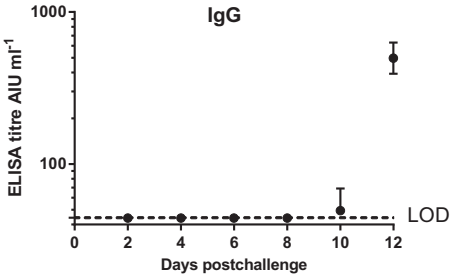

FIG 2 Serum IgG responses following challenge, measured by ELISA (mean + 1 SE, $n = 3$ to 5 macaques). Day 0, time of challenge with monkeypox virus. LOD, limit of detection (44.1 AIU ml^{-1}).

TABLE 3 Mean number of PFU of monkeypox virus in whole blood and throat swabs taken on different days postchallenge

Day postchallenge	Live virus PFU ml^{-1} (±SE)	
	Whole blood	Throat swab
2	<LOD[a]	25 ± 0
4	<LOD	$4.5 \times 10^2 \pm 4.3 \times 10^2$
6	<LOD	$1.9 \times 10^2 \pm 85$
8	<LOD	$1.4 \times 10^3 \pm 1.2 \times 10^3$
10	<LOD	$2.2 \times 10^2 \pm 1.9 \times 10^2$
12	<LOD	$6.4 \times 10^2 \pm 6.2 \times 10^2$

[a] <LOD, less than the limit of detection (250 PFU ml^{-1}).

infectious virus (PFU) above the limit of detection was detected in the blood on any of the days tested (Table 3).

Body tissues were assayed by real-time PCR, and on day 2, positive PCR results were restricted to the lungs (2.5×10^4 to 2.7×10^4 copies mg^{-1}); by day 4, this increased to 5.1×10^5 to 2.9×10^6 copies mg^{-1} (Fig. 4). On day 4, vDNA was also detected in the spleen and tonsils. By day 6, at least seven of the 13 tissues contained vDNA. The level of vDNA in the lungs remained high (3.7×10^6 to 5.7×10^6 copies mg^{-1}), while at least approximately 1×10^5 copies mg^{-1} of vDNA were detected in the spleen, tonsil, and tongue. By day 8, 9/13 tissues were positive for vDNA, including the kidney, heart, tongue, cerebrospinal fluid, spleen, and mediastinal lymph nodes. The concentration of virus in the tonsils (6×10^6 copies mg^{-1}) exceeded that in the lungs (3×10^6 copies mg^{-1}). Two animals in the "reserve group" were euthanized on humane grounds on day 8, and there was no difference in virological data between these two animals and the scheduled three animals. By day 10, the PCR values detected in the lungs decreased to 6.8×10^5 to 1.3×10^6 copies mg^{-1} (Fig. 4), although the concentration of vDNA in the tonsil was still high at 1.8×10^7 copies mg^{-1}. A decrease in viral load was apparent in all the animals on day 12, with values down to 1.1×10^4 to 3.8×10^5 copies mg^{-1} in the lungs (Fig. 4). This was consistent with clinical observations indicating that these animals were recovering.

Pathology. Histopathological changes and results of immunostaining are summarized in Table 4. On day 2 postchallenge, histological changes were restricted to respiratory bronchioles (Fig. 5a) in the lungs of two of three animals. They comprised occasional, small foci of dysplastic and sloughed cells. In immunostained sections, monkeypox antigen was present focally in all three animals, most frequently in the bronchioles and alveoli but occasionally in the epithelium of bronchi. Positive immunostaining was not observed in any other tissue on day 2.

On day 4 postchallenge, histological abnormalities were observed in the lungs of 3 animals. They were more numerous and developed than on day 2 postchallenge, comprising foci of epithelial necrosis and inflammation. In bronchioles, focal epithelial dysplasia, epithelial necrosis, and sloughing (Fig. 5b), with infiltration by neutrophils and occasionally eosinophils, were observed. Thickening of alveolar walls was seen diffusely in one animal and focally in another; a small number of alveoli were dilated. In the tracheobronchial lymph node of 1/3 animals, scattered foci of inflammatory cells, primarily histiocytes, were detected (Fig. 5c). Pathological changes were not observed in any other organ. Monkeypox antigen was detected by immunostaining in all lung lobes in all animals, more prominently than on day 2, located in the epithelium of bronchi (Fig. 5b inset), bronchioles, and alveolar walls. In the hilar (tracheobronchial) lymph node, positive staining was located in the outer cortex adjacent to the subcapsular sinus (Fig. 5c, inset). In addition, in the absence of histological changes, a few scattered positive cells were detected in the spleen (Fig. 5d) and submandibular lymph nodes of one animal and the lamina propria of the colon of another animal.

On day 6 postchallenge, severe lesions were noted in the lungs, comprising focal necrosis of airway epithelium and neutrophil infiltration, with lower airways affected more severely than upper airways (Fig. 5e). Diffuse and focal thickening of alveolar walls by macrophages and neutrophils was common, and some alveolar dilation was present. Peribronchial edema and periarterial edema, sometimes with infiltration by macrophages and neutrophils, were seen less frequently. Vascular lesions, comprising endothelial margination of macrophages and neutrophils, were seen occasionally. Focal necrosis with neutrophil infiltration was noted in the tracheobronchial lymph node, occurring in the outer cortex and subcapsular sinuses and infrequently in the medulla. In addition, lesions were detected in all animals in the tonsil and spleen and in the trachea/larynx of one of three animals. Lesions in the tonsil comprised focal necrosis of the crypt epithelium and/or lymphoid follicles, with neutrophil infiltration. In the spleen, focal necrosis with neutrophil infiltration was noted, most frequently in periarteriolar lymphoid sheaths. Immunostaining was positive, with a distribution similar to that for the lesions described above, including the spleen (Fig. 5f). In addition, scattered, positive staining was found in the colon and axillary lymph node in 1/3 animals, in the absence of histological changes.

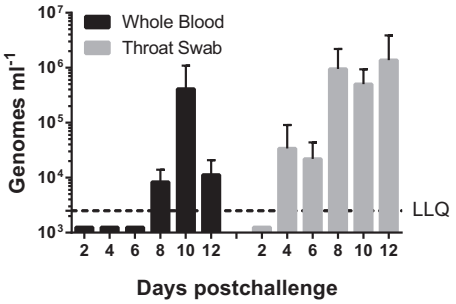

FIG 3 Mean number (+1 SD) of viral genomes (HA gene) as determined from qPCR in the blood and throat in samples taken following challenge with aerosolized monkeypox virus. The lower limit of quantification for qPCR (LLQ) was 2,500 genomes ml^{-1}.

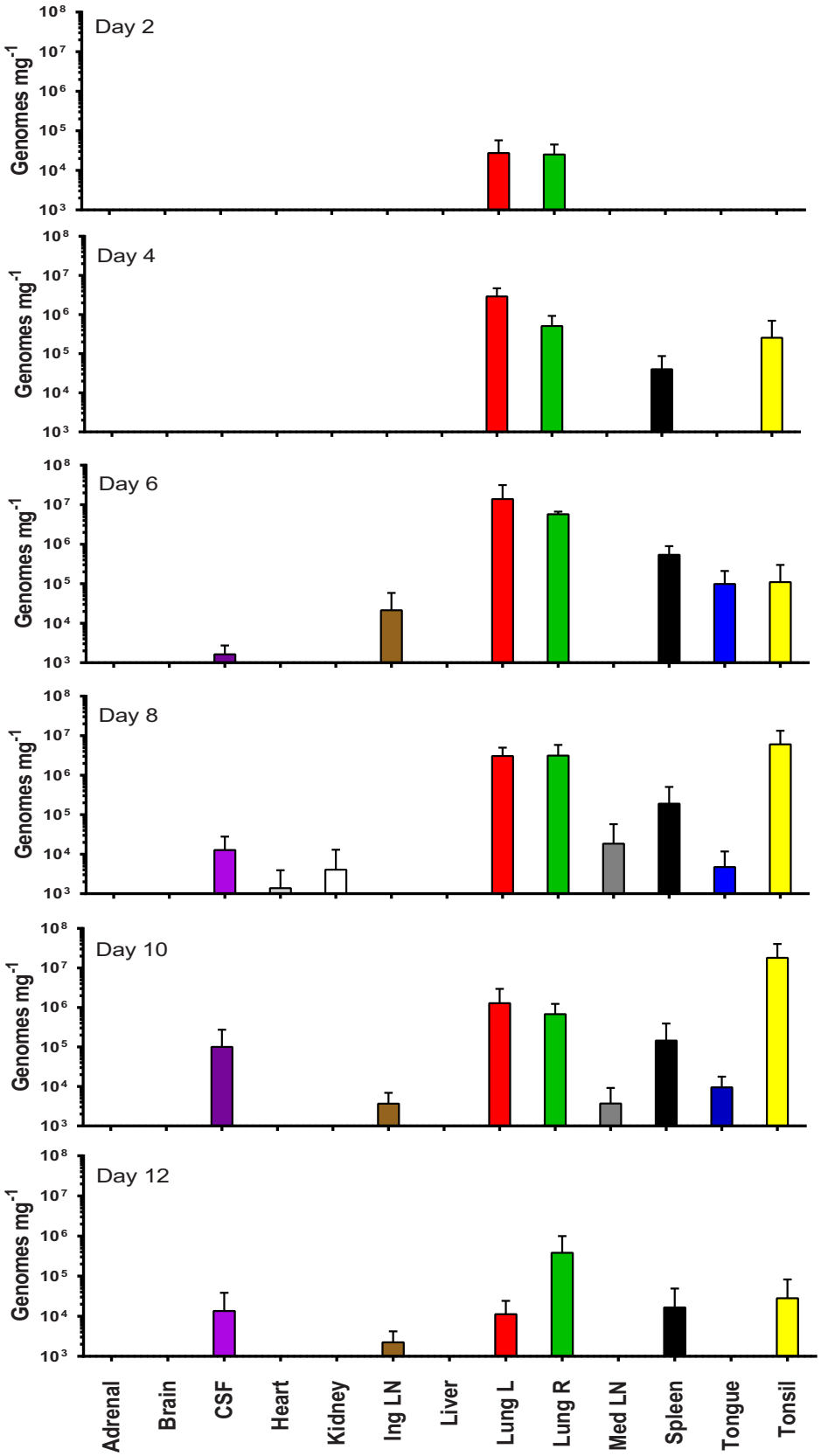

FIG 4 Viral load in tissues following challenge with monkeypox virus. The mean viral load (+1 SD), as determined by real-time PCR, in the tissues of animals taken at postmortem on different days of the study. For graphical purposes, the LLQ has been assigned 1,000 genomes mg^{-1} due to variability in the weights of tissue recovered at necropsy.

TABLE 4 Summary of the occurrence of monkeypox-related lesions and positive immunohistochemistry results in cynomolgus macaques following challenge with monkeypox virus[a]

Organ	No. of samples with positive H&E or IHC results/total no. of samples											
	Day 2		Day 4		Day 6		Day 8		Day 10		Day 12	
	H&E	IHC	H&E	IHC	H&E	IHC	H&E	IHC	H&E	IHC	H&E	IHC
Trachea/larynx	0/3	0/3	0/3	0/3	1/3	1/3	1/5	1/5	0/3	0/3	1/4	1/4
Lung RU	0/3	3/3	3/3	3/3	3/3	3/3	5/5	5/5	3/3	3/3	4/4	2/4
Lung RM	0/3	3/3	3/3	3/3	3/3	3/3	5/5	5/5	3/3	3/3	4/4	2/4
Lung RL	1/3	3/3	3/3	3/3	3/3	3/3	5/5	5/5	3/3	3/3	4/4	2/4
Lung LU	1/3	3/3	2/3	3/3	3/3	3/3	5/5	5/5	3/3	3/3	4/4	3/4
Lung LL	2/3	3/3	3/3	3/3	3/3	3/3	5/5	5/5	3/3	3/3	4/4	3/4
Hilar LN	0/2	0/2	1/3	2/3	3/3	3/3	4/5	4/5	1/3	2/3	2/3	1/4
Spleen	0/3	0/3	0/3	1/3	3/3	3/3	3/5	4/5	2/3	1/3	2/4	0/4
Tongue	0/3	0/3	0/3	0/3	0/3	0/3	2/5	2/5	0/3	0/3	0/3	0/3
Tonsil	0/3	0/3	0/3	0/3	3/3	3/3	3/3	3/3	2/2	2/2	0/2	0/2
Mandibular LN	0/3	0/3	0/2	1/2	2/2	2/2	2/5	3/5	1/3	1/3	0/3	0/3
Stomach	0/3	0/3	0/3	0/3	0/3	0/3	0/5	1/5	0/3	0/3	0/3	0/3
Ileum	0/3	0/3	0/3	0/3	0/3	0/3	0/3	0/3	0/3	0/3	0/3	0/3
Colon	0/3	0/3	0/3	1/3	0/3	1/3	1/5	2/5	1/3	1/3	0/3	0/3
Mesenteric LN	0/3	0/3	0/3	0/3	0/3	0/3	1/5	1/5	0/3	0/3	0/3	0/3
Skin	0/3	0/3	0/3	0/3	0/3	0/3	1/5	1/4	0/3	0/2	1/4	1/3
Inguinal LN	0/3	0/3	0/3	0/3	0/3	0/3	0/5	3/5	0/3	0/3	0/3	0/1
Axillary LN	0/3	0/3	0/3	0/3	0/3	1/3	0/3	0/2	0/3	0/3	0/3	0/2

[a] Lung RU, right upper lobe; lung RM, right middle lobe; lung RL, right lower lobe; lung LU, left upper lobe; lung LL, left lower lobe; LN, lymph node; H&E, hematoxylin and eosin; IHC, immunohistochemistry (to identify monkeypox virus antigens).

From days 8 to 10 postchallenge, lesions in the lung and other tissues attributed to monkeypox infection were severe and extensive. Distribution of positive immunostaining was widespread (Table 4).

In all three animals remaining on day 12 after challenge, occasional acute lesions were observed, but there was some evidence of early resolution that comprised cuboidal, nonciliated epithelial cells. Immunostained monkeypox antigen was still present in the respiratory tract, including in the hilar lymph node, but was not observed in the remaining tissues examined (Table 4).

DISCUSSION

When human efficacy studies are neither ethical nor feasible, the FDA may grant marketing approval of a new product, such as a vaccine, based upon the Animal Rule. Well-characterized animal models, however, are a requirement of this rule. This study characterized the early stages of monkeypox infection in cynomolgus macaques, using a dose of 10^5 PFU, delivered by the aerosol route. These early events have not been previously investigated in detail. Here, special emphasis was placed on examining the virological, immunological, and pathological changes in early infection.

Previous experiments examining monkeypox disease progression have monitored the clinical signs of disease until animals have reached a humane endpoint or have died in the study. This invariably happened 6 to 9 days after challenge, depending on the dose and route of challenge. In this work, a different approach was taken; animals were divided into groups and euthanized on designated days unless individuals were observed to have reached a humane endpoint. Thus, a mix of animals was studied; some had developed severe disease at the time of euthanasia, while some developed only mild disease. This approach has allowed the detailed study of the early events following challenge that were missing from studies based on animals with severe disease (22, 23).

Few studies have examined the immune response of cynomolgus macaques following exposure to aerosolized monkeypox virus. In this work, trends in the data showed a decrease in different immune cell populations early on in the course of the infection. Larger animal group sizes, however, are needed in order to confirm this statistically. Nevertheless, this could be indicative of immunosuppression, as the immunomodulatory effect of monkeypox virus has been previously observed by others (2, 31, 32). The rises in lymphocytes, in particular $CD8^+$ T cells, observed later in monkeypox infection, are likely to be the result of the host raising an adaptive immune response to the viral infection. Monocytes also increased above baseline levels on day 4 postinfection and again on days 8, 10, and 12. In this work, individual, circulating monocytes were not examined for infection with monkeypox virus; however, Zaucha and colleagues showed in their NHP studies that monocytic cells were immunopositive for poxviral antigen in a variety of organs and proposed that monkeypox virus spread initially via the lymph nodes and the mononuclear phagocytic/dendritic cell system (23).

Changes in the concentrations of circulating cytokines in the blood have been recorded in NHPs following challenge with different doses of monkeypox virus (5×10^4 to 5×10^7 PFU), via the intravenous and intrabronchial routes (8). Maximum mean peak fold changes in IFN-γ (8,028), IL-1ra (4,854), and IL-6 (3,207) were recorded on a variety of days (8). In this study, the mean peak changes in the biomarkers IFN-γ (1,322 pg ml^{-1}), IL-1ra (3,335 pg ml^{-1}), and IL-6 (570 pg ml^{-1}) occurred on day 8 postchallenge. The results of different studies are difficult to compare, because of the different ways data sets are presented and because different challenge doses and inoculation routes are used. However, it is clear IFN-γ, IL-1ra, and IL-6 play a role in the host response to monkeypox infection.

In this study, day 8 was the time when vDNA was detected in

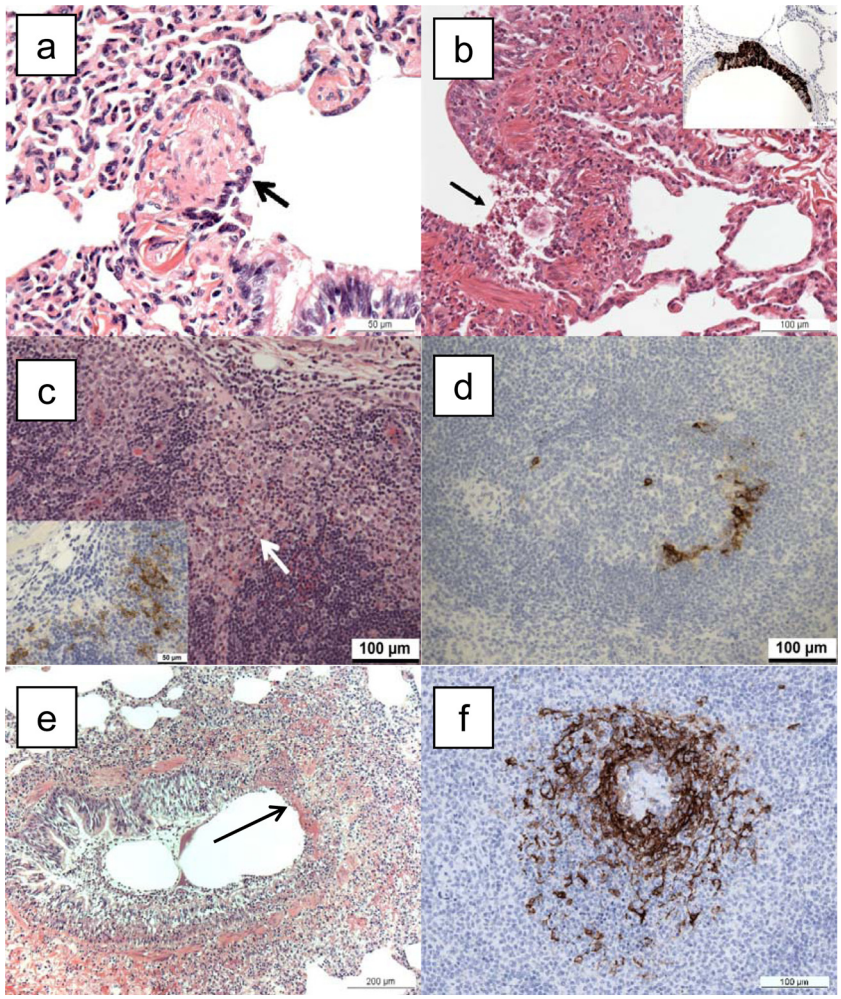

FIG 5 Histopathological changes associated with infection with monkeypox virus. (a) Lung, animal M965A, euthanized on day 2 postchallenge. Sloughing of respiratory bronchiolar epithelial cells (arrow) close to the junction with a bronchus. H&E. (b) Lung, animal M029F, euthanized on day 4 postchallenge. Focal epithelial cell necrosis (arrow), with sloughed cells and neutrophil infiltration at the junction of a bronchus and bronchiole. H&E. Inset, lung, animal I089K, euthanized on day 4 postchallenge. Focal, positive immunostaining of bronchial epithelium for monkeypox viral antigen. IHC. (c) Tracheobronchial lymph node, animal M029F, euthanized on day 4 postchallenge. Infiltration of superficial cortex by macrophages (arrow). HE. Inset, scattered, positively stained cells for monkeypox viral antigen. IHC. (d) Spleen, animal M293E, euthanized on day 4 postchallenge. Scattered, positively stained cells for monkeypox viral antigen in the white pulp. IHC. (e) Lung, animal M865B, euthanized 6 days postchallenge. Focal, bronchial epithelial necrosis (arrow). HE. (f) Spleen, animal I430G, euthanized on day 6 postchallenge. Positive immunostaining for monkeypox viral antigen in a periarteriolar lymphoid sheath (PALS) within the white pulp. IHC.

most tissues (9/13) and for death to most likely occur. It was also apparent that there was considerable animal-to-animal variation, and while the majority of the animals reached humane endpoints at approximately days 8 to 10, some survived the acute disease, as evidenced by the decline in the viral load in the blood and lung and tonsil tissues on day 12. The results of this experiment are similar to those reported by Nalca et al., in which, following an inhaled dose of 1.4×10^5 PFU, the mean time to death in cynomolgus macaques was 9 days (22). They also reported the peak viral load in blood (10^6 to 10^7 genomes ml^{-1}) was seen on day 10 postexposure; this was also noted on day 10 in this study (5×10^5 genomes ml^{-1}). Barnewall et al. also exposed two macaques to an aerosolized target dose of 1×10^5 PFU monkeypox virus; one died on day 8 and the other on day 9, and 2.7×10^5 to 3.6×10^5 genomes ml^{-1} were recorded in the blood on day 8 (24).

The histopathological and immunohistochemical findings in this study from animals examined on days 2, 4, and 6 postchallenge confirm earlier findings (23) and have identified features of pathogenesis not reported previously, to the authors' knowledge. Zaucha and colleagues studied cynomolgus macaques exposed to an aerosol of monkeypox virus that died or were euthanized 9 to 17 days after exposure (23). They concluded that the lower airway epithelium was the principal target, and the present study supports their proposition and additionally illustrates infection and lesions in these epithelia as early as 2 days after challenge. They proposed that tonsil, mandibular nodes, and mediastinal nodes were infected early. The findings of this study support their proposition; on day 4, 2/3 hilar nodes immunostained positively and 3/3 on day 6. On day 4, one of the two mandibular lymph nodes immunostained positively, and 2/2 were positive on day 6 when 3/3 tonsils were positive. Zaucha and colleagues (23) concluded that the spleen and gastrointestinal tract became infected later, but this was not supported by the findings of this study, which recorded immunostaining in 1/3 spleens on day 4 and 3/3 on day 6.

Positive immunostaining was present in the colon of 1/3 animals on day 4. The findings from animals euthanized on days 8, 10, and 12 after challenge were consistent with those of a previous study (23).

This work describes, for the first time, the sequence of early pathological events that occur following inhalation of 10^5 PFU monkeypox virus in cynomolgus macaques. Monkeypox virus vDNA was detected in the lungs 2 days postinfection, and by day 4 the virus was detected in the throat, tonsil, and spleen. Viral antigen was also detected by immunohistochemistry in the lungs, spleen, colon, and mandibular and hilar lymph nodes on day 4. From day 6, signs of acute disease were obvious and pox lesions appeared. In 1988, Fenner and colleagues inferred, from limited available information, that the clinical manifestations of naturally acquired smallpox in humans began after an incubation period of 7 to 17 days following exposure (33). The first febrile phase lasted for 3 to 4 days, followed by the appearance of a rash. Our model partially resembles some of the features of the human condition, which helps to bridge the gap in our understanding of variola virus infection and improves our understanding of monkeypox viral disease while at the same time further characterizing this important smallpox animal model, as required by the FDA's Animal Rule.

ACKNOWLEDGMENTS

This work was funded by the National Institute of Allergy and Infectious Diseases (contact NO1-AI-30062, task orders 03 and 04).

The views in the paper are of the authors and not necessarily those of the funding body.

We thank Robert Johnson, Thames Pickett, and Helen Schiltz for reviewing the manuscript. We thank Victoria Cox (DSTL) for advice about statistical analysis. We are grateful to Susan Gray for preparing the histology samples. We appreciate the technical assistance provided by Debbie Atkinson, Gemma McLuckie, Mel Davison, and Thomas Tipton. We are also very grateful to the Biological Investigations Group at the PHE, in particular Paul Yeates and Janice Pickersgill, for conducting the animal procedures.

REFERENCES

1. **Breman JG, Arita I.** 1980. The confirmation and maintenance of smallpox eradication. New Engl J Med **303:**1263–1273. http://dx.doi.org/10.1056/NEJM198011273032204.
2. **Stanford MM, McFadden G, Karupiah G, Chaudhri G.** 2007. Immunopathogenesis of poxvirus infections: forecasting the impending storm. Immunol Cell Biol **85:**93–102. http://dx.doi.org/10.1038/sj.icb.7100033.
3. **von Krempelhuber A, Vollmar J, Pokorny R, Rapp P, Wulff N, Petzold B, Handley A, Mateo L, Siersbol H, Kollaritsch H, Chaplin P.** 2010. A randomized, double-blind, dose-finding phase II study to evaluate immunogenicity and safety of the third generation smallpox vaccine candidate IMVAMUNE. Vaccine **28:**1209–1216. http://dx.doi.org/10.1016/j.vaccine.2009.11.030.
4. **Chapman JL, Nichols DK, Martinez MJ, Raymond JW.** 2010. Animal models of orthopoxvirus infection. Vet Pathol **47:**852–870. http://dx.doi.org/10.1177/0300985810378649.
5. **FDA.** 2002. New drug and biologics and drug products; evidence needed to demonstrate effectiveness of new drugs when human efficacy studies are not ethical or feasible. Fed Regist **67:**37988–37998.
6. **Damon IK.** 2011. Status of human monkeypox: clinical disease, epidemiology and research. Vaccine **29**(Suppl 4)**:**D54–D59. http://dx.doi.org/10.1016/j.vaccine.2011.04.014.
7. **Parker S, Buller RM.** 2013. A review of experimental and natural infections of animals with monkeypox virus between 1958 and 2012. Future Virol **8:**129–157. http://dx.doi.org/10.2217/fvl.12.130.
8. **Johnson RF, Dyall J, Ragland DR, Huzella L, Byrum R, Jett C, St Claire M, Smith AL, Paragas J, Blaney JE, Jahrling PB.** 2011. Comparative analysis of monkeypox virus infection of cynomolgus macaques by the intravenous or intrabronchial inoculation route. J Virol **85:**2112–2125. http://dx.doi.org/10.1128/JVI.01931-10.
9. **Earl PL, Americo JL, Wyatt LS, Eller LA, Whitbeck JC, Cohen GH, Eisenberg RJ, Hartmann CJ, Jackson DL, Kulesh DA, Martinez MJ, Miller DM, Mucker EM, Shamblin JD, Zwiers SH, Huggins JW, Jahrling PB, Moss B.** 2004. Immunogenicity of a highly attenuated MVA smallpox vaccine and protection against monkeypox. Nature **428:**182–185. http://dx.doi.org/10.1038/nature02331.
10. **Earl PL, Americo JL, Wyatt LS, Espenshade O, Bassler J, Gong K, Lin S, Peters E, Rhodes L, Jr, Spano YE, Silvera PM, Moss B.** 2008. Rapid protection in a monkeypox model by a single injection of a replication-deficient vaccinia virus. Proc Natl Acad Sci U S A **105:**10889–10894. http://dx.doi.org/10.1073/pnas.0804985105.
11. **Buchman GW, Cohen ME, Xiao Y, Richardson-Harman N, Silvera P, DeTolla LJ, Davis HL, Eisenberg RJ, Cohen GH, Isaacs SN.** 2010. A protein-based smallpox vaccine protects non-human primates from a lethal monkeypox virus challenge. Vaccine **28:**6627–6636. http://dx.doi.org/10.1016/j.vaccine.2010.07.030.
12. **Hirao LA, Draghia-Akli R, Prigge JT, Yang M, Satishchandran A, Wu L, Hammarlund E, Khan AS, Babas T, Rhodes L, Silvera P, Slifka M, Sardesai NY, Weiner DB.** 2011. Multivalent smallpox DNA vaccine delivered by intradermal electroporation drives protective immunity in non-human primates against lethal monkeypox challenge. J Infect Dis **203:**95–102. http://dx.doi.org/10.1093/infdis/jiq017.
13. **Huggins J, Goff A, Hensley L, Mucker E, Shamblin J, Wlazlowski C, Johnson W, Chapman J, Larsen T, Twenhafel N, Karem K, Damon IK, Byrd CM, Bolken TC, Jordan R, Hruby D.** 2009. Nonhuman primates are protected from smallpox virus or monkeypox virus challenges by the antiviral drug ST-246. Antimicrob Agents Chemother **53:**2620–2625. http://dx.doi.org/10.1128/AAC.00021-09.
14. **Jordan R, Goff A, Frimm A, Corrado ML, Hensley LE, Byrd CM, Mucker E, Shamblin J, Bolken TC, Wlazlowski C, Johnson W, Chapman J, Twenhafel N, Tyavanagimatt S, Amantana A, Chinsangaram J, Hruby DE, Huggins J.** 2009. ST-246 antiviral efficacy in a nonhuman primate monkeypox model: determination of the minimal effective dose and human dose justification. Antimicrob Agents Chemother **53:**1817–1822. http://dx.doi.org/10.1128/AAC.01596-08.
15. **Stittelaar KJ, van Amerongen G, Kondova I, Kuiken T, van Lavieren RF, Pistoor FH, Niesters HG, van Doornum G, van der Zeijst BA, Mateo L, Chaplin PJ, Osterhaus AD.** 2005. Modified vaccinia virus Ankara protects macaques against respiratory challenge with monkeypox virus. J Virol **79:**7845–7851. http://dx.doi.org/10.1128/JVI.79.12.7845-7851.2005.
16. **Stittelaar KJ, Neyts J, Naesens L, van Amerongen G, van Lavieren RF, Holy A, De Clercq E, Niesters HG, Fries E, Maas C, Mulder PG, van der Zeijst BA, Osterhaus AD.** 2006. Antiviral treatment is more effective than smallpox vaccination upon lethal monkeypox virus infection. Nature **439:**745–748. http://dx.doi.org/10.1038/nature04295.
17. **Goff AJ, Chapman J, Foster C, Wlazlowski C, Shamblin J, Lin K, Kreiselmeier N, Mucker E, Paragas J, Lawler J, Hensley L.** 2011. A novel respiratory model of infection with monkeypox virus in cynomolgus macaques. J Virol **85:**4898–4909. http://dx.doi.org/10.1128/JVI.02525-10.
18. **Saijo M, Ami Y, Suzaki Y, Nagata N, Iwata N, Hasegawa H, Iizuka I, Shiota T, Sakai K, Ogata M, Fukushi S, Mizutani T, Sata T, Kurata T, Kurane I, Morikawa S.** 2009. Virulence and pathophysiology of the Congo Basin and West African strains of monkeypox virus in non-human primates. J Gen Virol **90:**2266–2271. http://dx.doi.org/10.1099/vir.0.010207-0.
19. **Nagata N, Saijo M, Kataoka M, Ami Y, Suzaki Y, Sato Y, Iwata-Yoshikawa N, Ogata M, Kurane I, Morikawa S, Sata T, Hasegawa H.** 2014. Pathogenesis of fulminant monkeypox with bacterial sepsis after experimental infection with West African monkeypox virus in a cynomolgus monkey. Int J Clin Exp Pathal **7:**4359–4370.
20. **Fenner F, Henderson DA, Arita I, Jezek Z, Ladnyi ID.** 1988. The epidemiology of smallpox, p 169–208. *In* Smallpox and its eradication. WHO, Geneva, Switzerland.
21. **Henderson DA, Inglesby TV, Bartlett JG, Ascher MS, Eitzen E, Jahrling PB, Hauer J, Layton M, McDade J, Osterholm MT, O'Toole T, Parker G, Perl T, Russell PK, Tonat K.** 1999. Smallpox as a biological weapon: medical and public health management. Working Group on Civilian Biodefense. JAMA **281:**2127–2137.
22. **Nalca A, Livingston VA, Garza NL, Zumbrun EE, Frick OM, Chapman**

JL, Hartings JM. 2010. Experimental infection of cynomolgus macaques (*Macaca fascicularis*) with aerosolized monkeypox virus. PLoS One **5**(9)**:** e12880. http://dx.doi.org/10.1371/journal.pone.0012880.

23. **Zaucha GM, Jahrling PB, Geisbert TW, Swearengen JR, Hensley L.** 2001. The pathology of experimental aerosolized monkeypox virus infection in cynomolgus monkeys (*Macaca fascicularis*). Lab Invest **81:**1581–1600. http://dx.doi.org/10.1038/labinvest.3780373.
24. **Barnewall RE, Fisher DA, Robertson AB, Vales PA, Knostman KA, Bigger JE.** 2012. Inhalational monkeypox virus infection in cynomolgus macaques. Front Cell Infect Microbiol **2:**117. http://dx.doi.org/10.3389/fcimb.2012.00117.
25. **Hatch GJ, Graham VA, Bewley KR, Tree JA, Dennis M, Taylor I, Funnell SG, Bate SR, Steeds K, Tipton T, Bean T, Hudson L, Atkinson DJ, McLuckie G, Charlwood M, Roberts AD, Vipond J.** 2013. Assessment of the protective effect of Imvamune and Acam2000 vaccines against aerosolized monkeypox virus in cynomolgus macaques. J Virol **87:**7805–7815. http://dx.doi.org/10.1128/JVI.03481-12.
26. **United Kingdom Home Office.** 1989. Code of practice for the housing and care of animals used in scientific procedures. United Kingdom Home Office, London, United Kingdom. https://www.gov.uk/government/uploads/system/uploads/attachment_data/file/228831/0107.pdf.
27. **National Committee for Refinement, Reduction, and Replacement (NC3Rs).** 2006. Guidelines on primate accommodation, care, and use. NC3Rs, London, United Kingdom.
28. **Gussman R.** 1984. Note on the particle size output of Collison nebulizers. Am Ind Hyg Assoc J **45:**B8–B12.
29. **May K.** 1973. The Collison nebulizer. Description, performance and application. J Aerosol Sci **4:**235.
30. **Druett HA.** 1969. A mobile form of the Henderson apparatus. J Hyg **67:**437–448. http://dx.doi.org/10.1017/S0022172400041851.
31. **Rubins KH, Hensley LE, Relman DA, Brown PO.** 2011. Stunned silence: gene expression programs in human cells infected with monkeypox or vaccinia virus. PLoS One **6:**e15615. http://dx.doi.org/10.1371/journal.pone.0015615.
32. **Alzhanova D, Hammarlund E, Reed J, Meermeier E, Rawlings S, Ray CA, Edwards DM, Bimber B, Legasse A, Planer S, Sprague J, Axthelm MK, Pickup DJ, Lewinsohn DM, Gold MC, Wong SW, Sacha JB, Slifka MK, Fruh K.** 2014. T cell inactivation by poxviral B22 family proteins increases viral virulence. PLoS Pathog **10:**e1004123. http://dx.doi.org/10.1371/journal.ppat.1004123.
33. **Fenner F, Henderson DA, Arista I, Jezek Z, Ladnyi ID.** 1988. The clinical features of smallpox, p 1–68. *In* Smallpox and its eradication. WHO, Geneva, Switzerland.